



Cite this: *RSC Adv.*, 2017, 7, 17071

Experimental observation and quantum chemical investigation of thallium(I) (*Z*)-methanediazotate: synthesis of a long sought and highly reactive species†‡

Neeraj Singh,^a Benjamin Fiedler,^{*b} Joachim Friedrich^b and Klaus Banert^{*a}

For the first time, successful synthesis and characterisation of the missing (*Z*)-isomer of thallium(I) methanediazotate has been accomplished, utilising low-temperature NMR monitoring analysis. The title compound was synthesised from *N*-methyl-*N*-nitrosoourea and thallium(I) propoxide, under sub-ambient temperature conditions, as a highly moisture sensitive entity. Quantum chemical calculations, performed at the CCSD(T) level, depict excellent conformity to experimental results. Indeed, compared to its (*E*) counterpart, the formation of the title compound is thermodynamically less favoured, but preferred by means of kinetic control owing to a hindered isomerisation.

Received 20th January 2017
Accepted 17th February 2017

DOI: 10.1039/c7ra00872d

rsc.li/rsc-advances

Alkane diazotates^{1,2} have long been discussed as highly reactive species, generated in the *in vivo* metabolism of *N*-nitrosooureas, and are responsible for the alkylation of DNA, thereby, acting as potent carcinogens.³ Fixation of nitrous oxide (N₂O) by frustrated Lewis-pairs (FLP's)⁴ and *N*-heterocyclic carbenes⁵ also leads to the formation of diazotates. The high moisture sensitivity, exhibited by these entities, makes them extremely difficult to isolate and handle at room temperature. In spite of that, certain diazotates, such as **1**, **2** and **4–6**, have been isolated and characterised by the XRD technique,⁶ for example, potassium(I) (*Z*)-methanediazotate (**4**) (Scheme 1a). It is long known that configurational isomerism exists in the diazotates owing to the restricted rotation about the N–N bond, and that (*Z*)-isomers are highly reactive when compared to the corresponding (*E*)-isomers.

Particularly noteworthy are thallium(I) methanediazotates,⁷ of which heretofore only the (*E*)-isomer **1** was isolated and characterised by single crystal X-ray analysis, by Keefer *et al.* Molecule **1** was synthesised by the nitrosation of methylhydrazine in the presence of thallium(I) ethoxide (TlOEt) (Scheme 1b), as a highly crystalline material stable to hydrolysis, a property which is highly contrasting to other similar diazotates and explained by the possible covalent nature of the thallium(I) cation. The configuration was assigned by analogy

with the very few (*Z*)-isomers, obtained by utilising the base induced decomposition of *N*-alkyl-nitroso-*N*-acyl derivatives (Scheme 1b). However, the exact mechanism detailing the preference of a particular configurational isomer remains speculative, since contrasting theoretical reports⁸ exist about the type of the conformation of *N*-nitrosoourea **7** in solvents, and furthermore, no consideration of the solvent was taken into account in determination of the *anti/syn* existence. Keefer and coworkers,⁷ however, could not directly characterise thallium(I) (*Z*)-methanediazotate (**3**), citing its highly reactive nature, and that still remains a gap in the field of thallium diazotates as well as in the larger case of covalent metal diazotates.

We became interested in the synthesis of (*Z*)-methanediazotate **3** and also in the theoretical basis for the formation of this diazotate along with the possibility of (*Z*)-(E) isomerisation under solvation. Thallium(I) alkoxides^{7,9} are unique bases owing to their covalent character and solubility in a range of organic solvents, even at low-temperatures, which is quintessential for monitoring reactions by low-temperature NMR analysis. Therefore, ¹⁵N-labelled *N*-methyl-*N*-nitrosoourea (**7**) was synthesised and reacted with TlOEt at –40 °C in CD₂Cl₂, under constant monitoring by low-temperature NMR spectroscopy.¹⁰ In this case, we could only observe the doublet for CH₂N¹⁵N at δ = 3.34 with ³J(¹⁵N,¹H) ≈ 1.1 Hz in the ¹H NMR spectrum and a signal at δ = 14.17 in the corresponding ¹⁵N NMR spectrum. The identity of ¹⁵N-labelled diazomethane was further confirmed by ¹⁵N,¹H gHMBCAD and by comparison with literature known values.¹¹ This result is in complete agreement with the known methods for the synthesis of diazotates and the observed secondary products in the absence of electrophiles (Scheme 2).¹¹

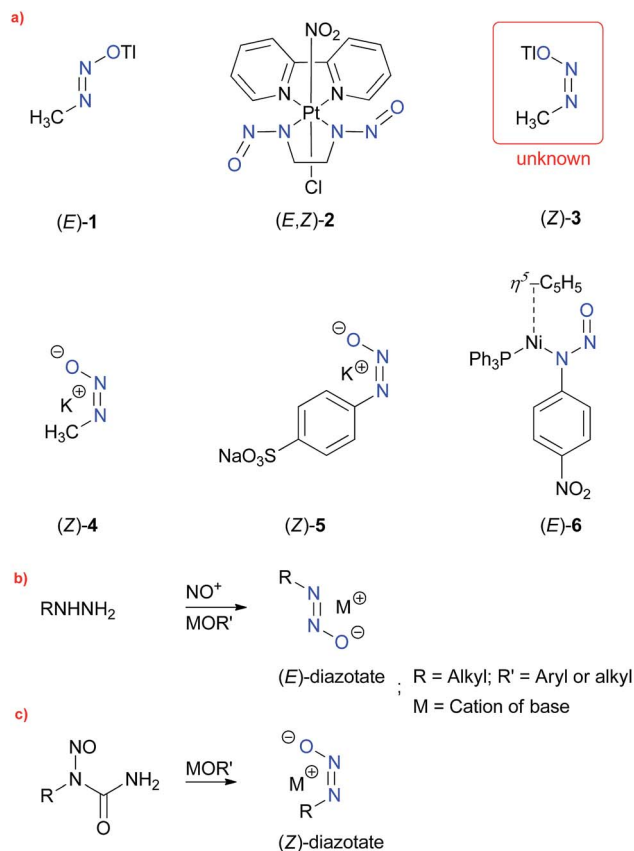
^aChemnitz University of Technology, Organic Chemistry, Strasse der Nationen 62, 09111 Chemnitz, Germany. E-mail: Klaus.banert@chemie.tu-chemnitz.de

^bChemnitz University of Technology, Theoretical Chemistry, Strasse der Nationen 62, 09111 Chemnitz, Germany. E-mail: benjamin.fiedler@chemie.tu-chemnitz.de

† Dedicated to Prof. V. K. Singh, Director, IISER Bhopal, India.

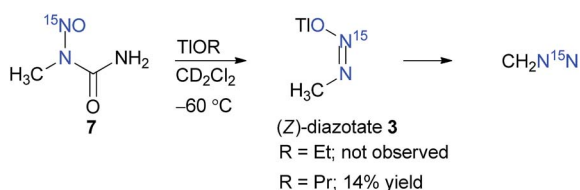
‡ Electronic supplementary information (ESI) available: Experimental procedures, spectroscopic data, copies of NMR spectra as well as coordinates and energies from quantum chemical calculations. See DOI: 10.1039/c7ra00872d





Scheme 1 (a) Reported diazotates (1–6) and unknown 4; (b) and (c) established methods for the syntheses of (E)- and (Z)-diazotates, respectively.

However, owing to our previous experience with thallium(I) alkoxides, it is known that TlOEt and thallium(I) propoxide (TlOPr)^{9a} react differently, probably because of their varying association nature.^{9,11} Therefore, to a solution of TlOPr (1.1 eq.) in CD₂Cl₂, maintained at –60 °C, was added *N*-nitrosourea 7 (10 mg), and the reaction was analysed by sub-ambient temperature ¹H and ¹⁵N NMR monitoring technique. To our pleasant surprise, along with the signals of CH₂N¹⁵N, we also obtained well-defined signals for thallium(I) (Z)-methanediazotate 3 in 14% yield (¹H NMR), with a doublet at δ = 3.17 with ³J(¹⁵N, ¹H) = 4.0 Hz in the ¹H NMR spectrum (Fig. 1), and a singlet at δ = 104.5 for the ¹⁵NOTl unit.¹⁰ The structure was further confirmed by ¹⁵N,¹H gHMBCAD 2D-NMR technique (Fig. 2). Compound 3 was stable for only a few hours at –60 °C, and decomposed completely to CH₂N¹⁵N (confirmed by NMR as mentioned



Scheme 2 Synthesis of diazotate 3 and subsequent decomposition to CH₂N¹⁵N.

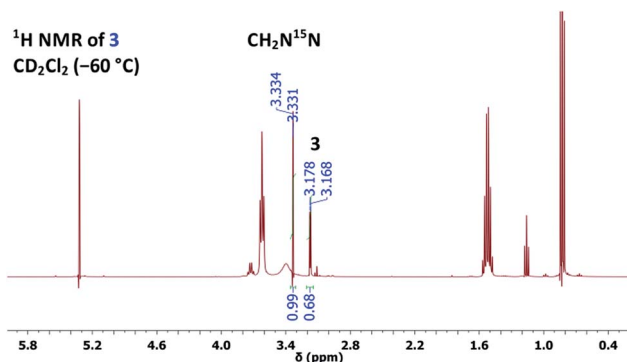


Fig. 1 ¹H NMR spectrum of (Z)-diazotate 3 and CH₂N¹⁵N.

before), which led to an increase of the total diazomethane yield from 31% to 43%. Since the ¹H NMR data and high stability of the corresponding (E)-diazotate⁷ 1 (δ = 3.43), stable at RT, contrasts significantly with the properties of the aforementioned species and because of the additional evidence obtained through ¹⁵N NMR as well as 2D-NMR experiments, the structure of the highly elusive (Z)-diazotate 3 is now confirmed.

Moreover, due to the existence of hindered rotation about N–N bond in *N*-nitrosoureas like 7 in different solvents, thereby, giving rise to *syn/anti* rotational isomers, it becomes essential to define the preference of a particular rotamer in special solvents. This existence of rotational isomerism plays an important role about the outcome of the stereochemistry of the thallium diazotates 1/3.

Therefore, we performed high-level quantum chemical calculations pertaining to the *anti/syn* conformational isomerism of *N*-nitrosourea 7 as well as the (Z)/(E) configurational isomerism of 3/1. Low-level theoretical calculations, without any consideration of solvent contributions, have been performed before, regarding to ionic diazotates, but they cannot be extended to covalent diazotates like 1/3.¹² Furthermore, by comparing the isomerisation energetics to the mechanisms for the TlOPr induced formation of both diazotates from the corresponding conformers of 7 (Fig. 3), we explain the occurrence of the thermodynamically less stable (Z)-isomer.

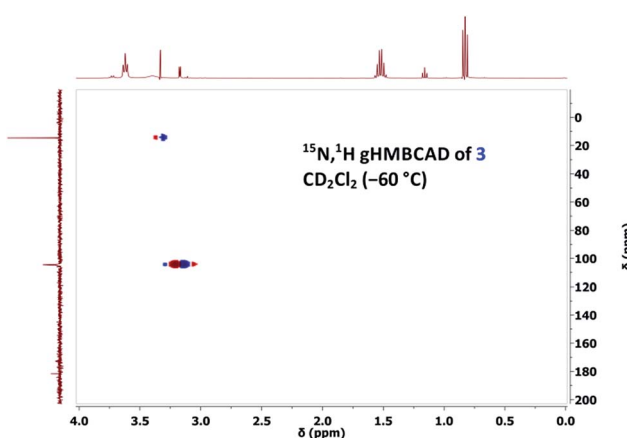


Fig. 2 ¹⁵N,¹H gHMBCAD NMR of (Z)-diazotate 3, with nitromethane as external reference.



The molecular geometries were optimised by TURBOMOLE V6.5,¹³ using RI-DFT¹⁴ with the PW6B95 functional,¹⁵ the D3 dispersion correction,¹⁶ the TZVPP basis set¹⁷ (def2-TZVPP with corresponding ECP for Tl¹⁸) as well as the COSMO solvation model ($\epsilon = 8.9$ for CD₂Cl₂).¹⁹ Numerical frequency analyses were performed to characterise the stationary points and to obtain the zero point vibrational energy.²⁰ The free module was used to calculate the Gibbs free energy contribution at the reaction temperature (-60°C). We also performed CCSD(T)/cc-pVXZ²¹ ($X = \text{T, Q}$) calculations (with pseudopotential for Tl²²) and a subsequent CBS(34) extrapolation²³ according to eqn (1) and (2) as well as CCSD(T)(F12)/cc-pVTZ-F12 (ref. 24) (aug-cc-pwCVTZ-PP basis for Tl²²) calculations to obtain highly accurate electronic energies. Additionally, we applied the focal-point method in eqn (3), using an MP2 increment to approach the CBS limit.

$$E_{\text{HF}}^{(XY)} = \frac{e^{-6.3\sqrt{Y}}E_{\text{HF}}^{(X)} - e^{-6.3\sqrt{X}}E_{\text{HF}}^{(Y)}}{e^{-6.3\sqrt{Y}} - e^{-6.3\sqrt{X}}} \quad (1)$$

$$E_{\text{corr}}^{(XY)} = \frac{X^3E_{\text{corr}}^{(X)} - Y^3E_{\text{corr}}^{(Y)}}{X^3 - Y^3} \quad (2)$$

$$E_{\text{foT/TZ}} = E_{\text{CCSD(T)}}^{\text{cc-pVTZ}} + (E_{\text{MP2-F12}}^{\text{cc-pVTZ-F12}} - E_{\text{MP2}}^{\text{cc-pVTZ}}) \quad (3)$$

With the single-point energy E_M , obtained by method M , and a Gibbs free energy contribution $G_{-60^\circ\text{C}}$ as well as a COSMO solvation correction ΔE_{solv} , both at the PW6B95-D3/TZVPP level, the total Gibbs free energy of a structure is obtained as:

$$G = E_M + G_{-60^\circ\text{C}} + \Delta E_{\text{solv}} \quad (4)$$

$$\Delta E_{\text{solv}} = E_{\text{COSMO}} - E_{\text{noCOSMO}} \quad (5)$$

Table 1 Activation (ΔG_{act}) and reaction (ΔG_{react}) Gibbs free energies for the *anti-syn* isomerisation of 7 and the (*Z*)-(E) isomerisation from 3 to 1. All energies are in kJ mol⁻¹ and method (M) refers to the calculation of the electronic energy

	Method M	DFT ^a	foT/TZ ^b	CBS(34) ^c	TZ-F12 ^d
<i>anti</i> -7 \rightarrow <i>syn</i> -7	ΔG_{act}	+103.2	+89.8	+91.5	+90.8
	ΔG_{react}	+20.7	+18.6	+18.9	+18.9
3 \rightarrow 1	ΔG_{act}	+176.7	+191.4	+192.2	+192.8
	ΔG_{react}	-17.8	-14.0	-16.7	-15.1

^a PW6B95-D3/TZVPP. ^b According to eqn (3), Tl: aug-cc-pwCVTZ-PP basis instead of cc-pVTZ-F12. ^c CBS(34) extrapolated CCSD(T)/cc-pVXZ according to eqn (1) and (2) with $X = 3$, $Y = 4$. ^d CCSD(T)(F12)/cc-pVTZ-F12, Tl: aug-cc-pwCVTZ-PP basis instead of cc-pVTZ-F12.

As shown in Table 1, the reaction energy (ΔG_{react}) for the *anti-syn* isomerisation of 7 is positive, representing the higher stability of the *anti*-rotamer. In contrast, the (*Z*)-diazotate 3, which yields from the *anti*-rotamer, is less stable than the (*E*) form. Indeed, the experimental results show the formation of the (*Z*) isomer, which excludes a thermodynamic reaction control (Fig. 3).

Furthermore, the activation barrier (ΔG_{act}) for the formation of the *syn*-rotamer is around 90 kJ mol⁻¹ and therefore rather large, representing the hindered rotation. However, the direct isomerisation of 3 to 1 needs significantly more activation (>190 kJ mol⁻¹) and can thus be excluded. Also, the covalent nature of the Tl-X ($X = \text{O, N}$) bond is supported by the Tl-O bond length in (*Z*)-diazotate 3 (2.42 Å; Fig. 4), in accordance with published results.

Considering the different highly accurate CCSD(T) methods to approach the complete basis set (CBS) limit, the relative energies of all three (Table 1) are in perfect agreement. Hence, the most efficient of them, the focal-point method in eqn (3),

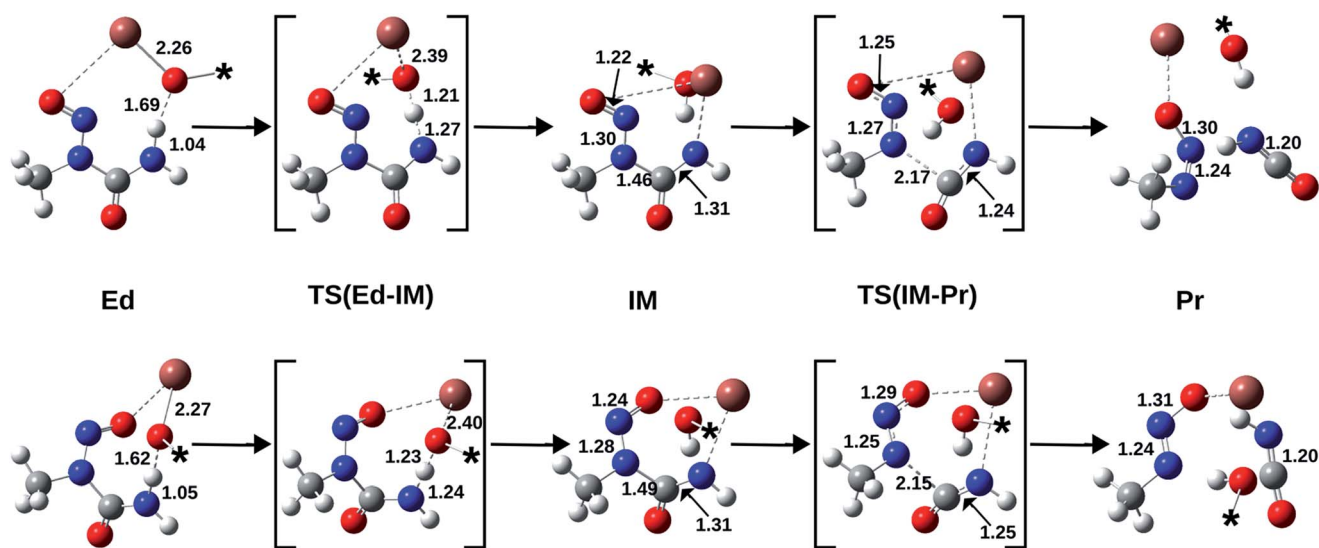


Fig. 3 Molecular structures, optimised with PW6B95-D3/TZVPP and COSMO ($\epsilon = 8.9$), for the reactions *anti*-7 \rightarrow 3 (top) and *syn*-7 \rightarrow 1 (bottom). Bond lengths (Å) have been depicted and the asterisk (*) represents the *n*-propyl group, which has been omitted for clear representation. Atoms are H (white), C (grey), N (blue), O (red), Tl (brown).



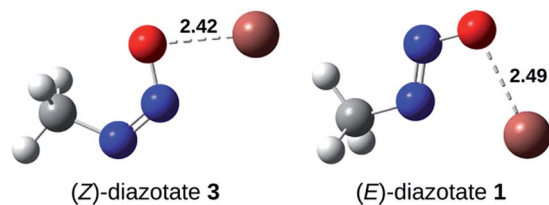


Fig. 4 Molecular structures, optimised with PW6B95-D3/TZVPP and COSMO ($\epsilon = 8.9$), of both thallium(I) diazotate conformers. The lengths (Å) of the Tl–O bonds are shown. Atoms are H (white), C (grey), N (blue), O (red), Tl (brown).

provides a suitable accuracy and expensive CCSD(T)/cc-pVQZ or CCSD(T)-F12/cc-pVTZ-F12 calculations are not necessary for the more extended model system, which is used for the reaction mechanisms.

Therefore, we modelled the mechanisms for the formation of **3** (respectively **1**) from *anti*-**7** (respectively *syn*-**7**) by using the focal-point method (Fig. 5). Again, the higher stability of the *anti*-educt and the lower one of the (*Z*)-product can be seen. Furthermore, the first reaction step, *i.e.* deprotonation of the urea by propoxide, is exothermic with a very low barrier in both cases. In contrast, the second step, *i.e.* the N–C bond cleavage, is endothermic for the (*Z*)-isomer and slightly exothermic for (*E*). However, this second step is rate-determining as it provides clearly larger activation energies of about 58 kJ mol⁻¹ for (*E*) and 82 kJ mol⁻¹ for (*Z*).

For completeness, we also calculated the rotation barrier for the intermediate (IM) of the reaction, *i.e.* the deprotonated *N*-nitroso-urea, and obtained 126 kJ mol⁻¹. Thus, if an isomerisation took place, it would occur at the educt step, as intermediate and product structure provide significantly higher rotation barriers. However, the barrier for the isomerisation of *anti*-**7** (≈ 90 kJ mol⁻¹) is still larger than the rate-determining step of the formation of **3** from *anti*-**7** (≈ 82 kJ mol⁻¹). Thus, the formation of the thermodynamically less stable (*Z*)-diazotate **3** can be explained by kinetic reaction control.

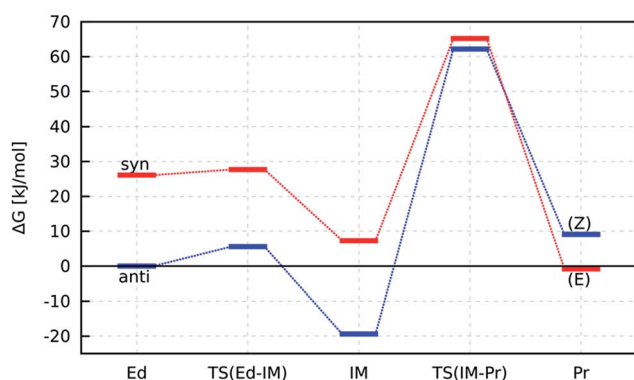


Fig. 5 Energy pathways for the reactions *anti*-**7** \rightarrow **3** (blue) and *syn*-**7** \rightarrow **1** (red). Gibbs free energies are calculated with the focal-point method (eqn (3)) for E_M respectively with PW6B95-D3/TZVPP ($G_{-60^\circ\text{C}}$, ΔE_{soln}) and shown relative to *anti*-**7**.

Conclusions

In summary, synthesis and characterisation of the elusive thallium(I) *Z*-diazotate **3** has been achieved for the first time. It was generated as a highly temperature and moisture sensitive entity by TIOPr induced decomposition of *N*-nitroso-urea **7**. The structure of the title compound has been confirmed unambiguously by ¹H NMR, ¹⁵N NMR and ¹⁵N,¹H gHMBCAD NMR spectroscopic analytical technique. The decomposition of (*Z*)-diazotate **3** to CH₂N¹⁵N, also confirms the general rule about the decomposition of other known (*Z*)-diazotates to diazomethane, in the presence of a base. Quantum chemical calculations, performed at the CCSD(T) level, reveal a kinetic, rather than a thermodynamic control, for the mechanism of the (*Z*)-diazotate **3** formation. Indeed, the (*Z*)-diazotate is thermodynamically less stable than the (*E*) form, but generated from the more stable *anti*-conformer of nitroso-urea **7**. Furthermore, the *anti*/*syn* rotational isomerisation is hindered and features even a larger activation energy than the rate-determining step within the formation of title compound **3**.

N-Methyl-*N*-nitroso-urea is a highly potent carcinogen, therefore, great precautions should be taken while handling it. Thallium(I) propoxide is a toxic compound and should be handled in accordance with safety protocols. Thallium (*E*)-diazotate can also lead to spontaneous explosions,⁷ therefore great care must be exercised while handling the highly reactive (*Z*)-diazotate.

Acknowledgements

We are grateful to Dr M. Hagedorn for his assistance with low-temperature NMR measurements. N. S. thanks DAAD (Deutscher Akademischer Austauschdienst) for a PhD fellowship. B. F. thanks the DFG Research Group FOR 1497 for financial support.

Notes and references

- R. A. Moss, *Acc. Chem. Res.*, 1974, **7**, 421–427.
- (a) P. Grieffs, *Justus Liebigs Ann. Chem.*, 1866, **137**, 39–91; (b) A. Wohl, *Ber. Dtsch. Chem. Ges.*, 1892, **25**, 3631–3634; (c) A. Engler, *Ber. Dtsch. Chem. Ges.*, 1900, **33**, 2188–2190; (d) K. J. P. Orton, *J. Chem. Soc.*, 1903, **83**, 796–814; (e) E. Müller and H. Haiss, *Chem. Ber.*, 1963, **96**, 570–583; (f) E. H. White, T. J. Ryan and K. W. Field, *J. Am. Chem. Soc.*, 1972, **94**, 1360–1361; (g) E. Müller, H. Haiss and W. Rundel, *Chem. Ber.*, 1960, **93**, 1541–1552; (h) E. Müller, W. Hoppe, H. Hagenmaier, H. Haiss, R. Huber, W. Rundel and H. Suhr, *Chem. Ber.*, 1963, **96**, 1712–1719.
- (a) W. P. Tong and D. B. Ludlum, *Biochem. Pharmacol.*, 1979, **28**, 1175–1179; (b) W. P. Tong, M. C. Kirk and D. B. Ludlum, *Cancer Res.*, 1982, **42**, 3102–3105; (c) J. A. Montgomery, *Cancer Treat. Rep.*, 1976, **60**, 651–664; (d) B. Singer, *Nature*, 1976, **264**, 333–339; (e) C. T. Gombar, W. P. Tong and D. B. Ludlum, *Biochem. Biophys. Res. Commun.*, 1979, **90**, 878–882; (f) J. D. Scribner and G. P. Ford, *Cancer Lett.*, 1982, **16**, 51–56; (g) K. K. Park, M. C. Archer and



- J. S. Wishnok, *Chem.-Biol. Interact.*, 1980, **29**, 139–144; (h) K. Morimoto, A. Tanaka and T. Yamaha, *Carcinogenesis*, 1983, **4**, 1455–1458.
- 4 E. Otten, R. C. Neu and D. W. Stephan, *J. Am. Chem. Soc.*, 2009, **131**, 9918–9919.
- 5 A. G. Tskhovrebov, E. Solari, M. D. Wodrich, R. Scopelliti and K. Severin, *Angew. Chem., Int. Ed.*, 2012, **51**, 232–234.
- 6 (a) W. A. Freeman, *J. Am. Chem. Soc.*, 1983, **105**, 2725–2729; (b) R. Huber, R. Langer and W. Hoppe, *Acta Crystallogr.*, 1965, **18**, 467–473; (c) L. Malatesta, G. La Monica, M. Manassero and M. Sansoni, *Gazz. Chim. Ital.*, 1980, **110**, 113–121; (d) N. W. Alcock, P. D. Goodman and T. J. Kemp, *J. Chem. Soc., Perkin Trans. 2*, 1980, 1093–1095; (e) F. J. Lalor, T. J. Desmond, G. Ferguson and P. Y. Siew, *J. Chem. Soc., Dalton Trans.*, 1982, 1981–1985.
- 7 L. K. Keefer, S.-m. Wang, T. Anjo, J. C. Fanning and C. S. Day, *J. Am. Chem. Soc.*, 1988, **110**, 2800–2806.
- 8 (a) A.-M. Sapse, G. Snyder and L. Osorio, *Cancer Res.*, 1984, **44**, 1904–1907; (b) N. Nakayama and O. Kikuchi, *J. Mol. Struct.: THEOCHEM*, 2001, **536**, 213–218.
- 9 (a) P. J. Burke, R. W. Matthews and D. G. Gillies, *J. Chem. Soc., Dalton Trans.*, 1980, 1439–1442; (b) C. Janiak, *Coord. Chem.*, 1997, **163**, 107–216.
- 10 See ESI for further details.†
- 11 K. Banert, N. Singh, B. Fiedler, J. Friedrich, M. Korb and H. Lang, *Chem. – Eur. J.*, 2015, **21**, 15092–15099.
- 12 J. W. Lown, M. S. Chauhan, R. R. Koganty and A.-M. Sapse, *J. Am. Chem. Soc.*, 1984, **106**, 6401–6408.
- 13 R. Ahlrichs, M. Bär, M. Häser, H. Horn and C. Kölmel, *Chem. Phys. Lett.*, 1989, **162**, 165–169.
- 14 (a) O. Treutler and R. Ahlrichs, *J. Chem. Phys.*, 1995, **102**, 346–354; (b) K. Eichkorn, O. Treutler, H. Öhm, M. Häser and R. Ahlrichs, *Chem. Phys. Lett.*, 1995, **242**, 652–660; (c) K. Eichkorn, F. Weigend, O. Treutler and R. Ahlrichs, *Theor. Chem. Acc.*, 1997, **97**, 119–124.
- 15 Y. Zhao and D. G. Truhlar, *J. Phys. Chem. A*, 2005, **109**, 5656–5667.
- 16 (a) S. Grimme, J. Antony, S. Ehrlich and H. Krieg, *J. Chem. Phys.*, 2010, **132**, 154104; (b) S. Grimme, S. Ehrlich and L. Goerigk, *J. Comput. Chem.*, 2011, **32**, 1456–1465.
- 17 F. Weigend, M. Häser, H. Patzelt and R. Ahlrichs, *Chem. Phys. Lett.*, 1998, **294**, 143–152.
- 18 F. Weigend and R. Ahlrichs, *Phys. Chem. Chem. Phys.*, 2005, **7**, 3297–3305.
- 19 A. Klamt and G. Schüürmann, *J. Chem. Soc., Perkin Trans. 2*, 1993, 799–805.
- 20 P. Deglmann, F. Furche and R. Ahlrichs, *Chem. Phys. Lett.*, 2002, **362**, 511–518.
- 21 T. H. Dunning Jr, *J. Chem. Phys.*, 1989, **90**, 1007–1023.
- 22 (a) K. A. Peterson, *J. Chem. Phys.*, 2003, **119**, 11099–11112; (b) B. Metz, M. Schweizer, H. Stoll, M. Dolg and W. Liu, *Theor. Chem. Acc.*, 2000, **104**, 22–28; (c) K. A. Peterson and K. E. Yousaf, *J. Chem. Phys.*, 2010, **133**, 174116; (d) C. Hättig, G. Schmitz and J. Kofmann, *Phys. Chem. Chem. Phys.*, 2012, **14**, 6549–6555.
- 23 (a) S. J. Zhong, E. C. Barnes and G. A. Petersson, *J. Chem. Phys.*, 2008, **129**, 184116; (b) A. Halkier, T. Helgaker, P. Jørgensen, W. Klopper, H. Koch, J. Olsen and A. K. Wilson, *Chem. Phys. Lett.*, 1998, **286**, 243–252.
- 24 (a) D. P. Tew, W. Klopper, C. Neiss and C. Hättig, *Phys. Chem. Chem. Phys.*, 2007, **9**, 1921–1930; (b) H. Fliegl, W. Klopper and C. Hättig, *J. Chem. Phys.*, 2005, **122**, 084107; (c) K. A. Peterson, T. Adler and H.-J. Werner, *J. Chem. Phys.*, 2008, **128**, 084102.

